The Virtual Double Slit Experiment

THESIS

submitted in partial fulfillment of the
requirements for the degree of

BACHELOR OF SCIENCE
in
PHYSICS

Author :	M.J. Hylkema
Student ID :	s1724002
Supervisor :	Dr. W. Löffler
Second corrector :	Dr. ir. P.S.W.M. Logman

Leiden, The Netherlands, July 6, 2021

The Virtual Double Slit Experiment

M.J. Hylkema

Huygens-Kamerlingh Onnes Laboratory, Leiden University
P.O. Box 9500, 2300 RA Leiden, The Netherlands

July 6, 2021

Abstract

This report is on the simulation of the double slit experiment. Diffraction calculations will be used to create a simulated version of the experiment in virtual reality in order to accommodate the growing number of first year physics students. The parameters for the double slit aperture and light source in the simulations are equal to those in the physical experiment. We calculate the diffraction patterns behind the double slit aperture using the Fresnel approximation on Kirchhoff's Integral Theorem. The diffraction integrals are either solved brute-force (by for-loop) or using a fast Fourier transform. With the latter approach, the simulations were made in two dimensions and the different components could be rotated in order to simulate the misalignment of the setup in the physical experiment.

Contents

Chapter 1

Introduction

The wave-particle duality of light is almost impossible to imagine, but can be easily demonstrated in a university lab. Light was regarded as particles before Young's double slit experiment in 1802 [18]. In this experiment, a beam of particles travels through a double slit before hitting a screen. The arrival of each separate particle can be recorded at the screen. The wave nature of the light causes the particles to interfere, and light and dark fringes that can be observed on the screen [10].

Young's double slit experiment is one of the experiments performed by first year physics students at Leiden University. However, more and more bachelor students enroll each year and space is limited. On top of the limited space, less students are allowed in the already confined lab due to the outbreak of COVID-19 [14]. The university is improving their remote education, and one way Leiden University is trying to accommodate students is by improving the remote physics experiments of the first year course 'Experimentele Natuurkunde' (EN).

Together with a company called VR Lab, the goal of this Bachelor Research Project is to simulate the double slit experiment in 3D. These simulations will be used by VR Lab to create a virtual reality environment where first year students can practice and prepare the double slit experiment at home. To simulate such an optical experiment, it is critical to understand what happens to light from the moment it leaves the laser, until it hits the screen and forms a diffraction pattern. Therefore, we will be addressing several approaches of how to calculate the diffraction pattern.

The goal of our Bachelor Research Project is to numerically calculate the diffraction pattern behind a double slit, using various methods and to investigate which is the best option. We will be looking at the analytical formula for diffraction behind a double slit, Fraunhofer diffraction, Fresnel diffraction and the Rayleigh Sommerfeld diffraction integral. Also, we will be comparing our numerical simulations to simulations made with "Diffractio, python module for diffraction and interference optics" [13].

In order to use the above-mentioned methods, first we will look at the theory and approximations necessary to implement said methods. To start, we will examine the double slit experiment using analytic propagation and assess the analytical formula. Then we will work on the derivation from the wave equation of light to the aforementioned diffraction formulas and theories: Fresnel and Fraunhofer diffraction, we will also discuss the difference between the Fresnel-Kirchhoff diffraction formula and the Rayleigh Sommerfeld diffraction integral. We will close the chapter on the theory by eventually deriving the analytical formula for the diffraction behind the double slit, which was mentioned at the start of Chapter 2.

In the next chapter, we will walk through the methods of our double slit experiment and results. Here, we also established the parameters for the simulations and numerical calculations. In chapter 4, the simulations are discussed. A comparison is made between the Diffractio simulations and our own numerical simulations using NumPy [8]. It is also analyzed which method works best for our purpose. In the final chapter, a summary is given and an outlook for future projects.

Chapter 2

Theoretical Background

In this chapter the foundations for the rest of the report are provided. First the concept of diffraction is explained using the Hugyens-Fresnel principle. Then, the analytical formula for the diffraction behind the double slit aperture is provided. Finally, the different diffraction integrals are derived from the wave equation of light. We will look at Rayleigh-Sommerfeld diffraction and then walk through the approximations of Fresnel and Fraunhofer diffraction. With the latter we will prove the validity of the analytical formula. In our further calculations, we denote the imaginary number i by j, since j is used in Python.

2.1 Diffraction

When a wave passes through obstacles such an aperture, its behavior cannot only be described in terms of light rays; photons that propagate along straight lines. With this assumption, light that falls on the edge of a non-reflective opaque screen gives a sharply defined shadow, the geometrical shadow. However, this is not observed in optical experiments. It is observed that the light propagates to the screen and enters the geometrical shadow of the opaque screen. This creates a diffraction pattern when it bends around the edge of the opaque screen [1].

Diffraction patterns can be analyzed using Huygens's principle. This principle states that every point of a wave front can be considered a secondary source of wavelets that spread out in all directions with the same speed as the propagation of the wave. The position of the wave front at a later time is the envelope of secondary waves at that time. If one wants to find the resultant displacement at any point, you combine all the individual displacements produced by the secondary waves and use the superposition principle [10]. Huygens published his principle in 1690, and Fresnel improved it later, hence later called Huygens-Fresnel principle [1].

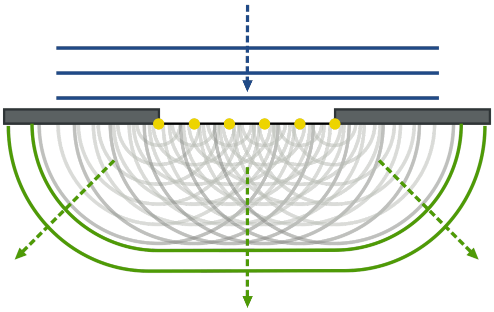

Figure 2.1: *Diffraction analyzed using Huygens's principle. The blue lines represent an incident plane. The yellow dots are the secondary wavelets. The green wave is the superposition of the displacements of these secondary wavelets [16].*

2.2 Principle Optics

Young's double slit was the first experiment to demonstrate the interference of light [9]. In the original experiment, sunlight was used as the light source, passed through a pinhole. Nowadays, a monochromatic coherent light source, such as a laser, is used in the most basic versions. This light source illuminates an aperture consisting of two narrow slits S_1 and S_2, as one can see in Figure 2.2. A screen can be placed at a distance z behind the aperture and a pattern of dark and light fringes can be seen [12]. The light fringes are the locations were light arrives in phase and interferes constructively. Dark fringes are located were light destructively interferes [10]. The key to obtain this pattern is to use mutually coherent light. Therefore, today we use a laser, but Young used a pinhole which emits monochromatic cylindrical wave fronts [7].

To simplify the analysis of the interference pattern seen on the screen we assume that the distance R between the aperture and the screen is much larger than the distance between the two slits in the aperture d, so $R >> d$. Then we can say that the rays coming from S_1 and S_2 are nearly parallel. The difference in path length between rays from S_1 and S_2 is given by [7]:

$$r_2 - r_1 = d \sin\theta \tag{2.1}$$

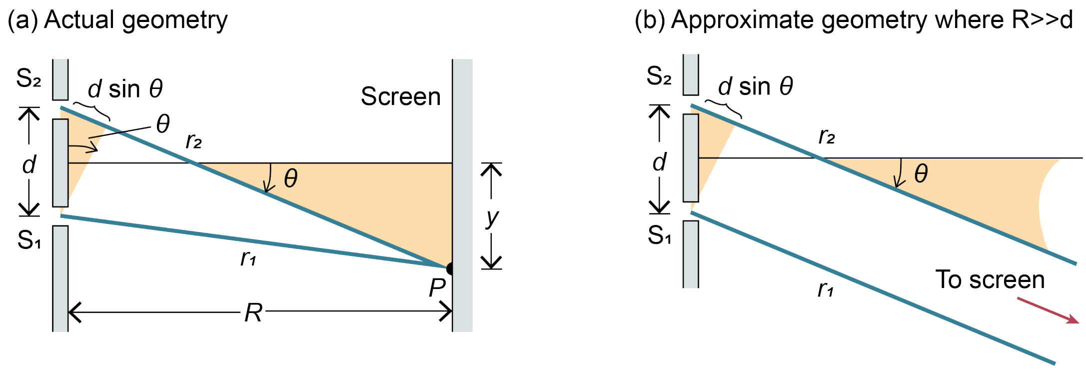

Figure 2.2: *Schematic drawing of situation behind double slit [10]. On the left one can see the actual geometry, and on the right an approximation is made; R ¿¿ d.*

Here d is the distance between the two slits, and θ is the angle between a line from the slits to screen. The intensity of the interference pattern on position y on the screen is:

$$I(y) = I_0 \cos^2(\frac{\pi d}{\lambda} \sin\theta) \tag{2.2}$$

In this equation λ is the wavelength of the light. The intensity on the screen has minimums and maximums. There is a maximum when: $d \sin\theta = m\lambda$. In the far field: $d << R$ so $\theta << 1$, this means that the positions of the maximums on the y-axis are given by:

$$y_m = R\frac{m\lambda}{d} \tag{2.3}$$

The distance between the different maximums Δy is given by $R\lambda/d$. Or in terms of the angle θ:

$$\Delta\theta \approx \frac{2\pi}{kd} = \frac{\lambda}{d} \tag{2.4}$$

where $k = \frac{\omega}{c}$, also known as the wavenumber.

Apart from this interference, one also has to take the finite width of the slits into account. This results in the following formula of the intensity of the diffraction pattern on position y [10],

$$I(y) = I_0 \left(\frac{\sin[\pi a(\sin\theta)/\lambda]}{\pi a(\sin\theta)/\lambda}\right)^2 \cos^2(\frac{\pi d}{\lambda} \sin\theta) \tag{2.5}$$

All the parameters are the same as in the previous equations, and a is the width of one slit. The extra term in Eq. 2.5 compared to Eq. 2.2 causes an envelope around the interference pattern. This sinc-function describes the diffraction pattern caused by a single slit. In Figure 2.3 we show the single slit diffraction pattern and double slit diffraction pattern. One can clearly see the single slit diffraction envelope in the double slit diffraction pattern.

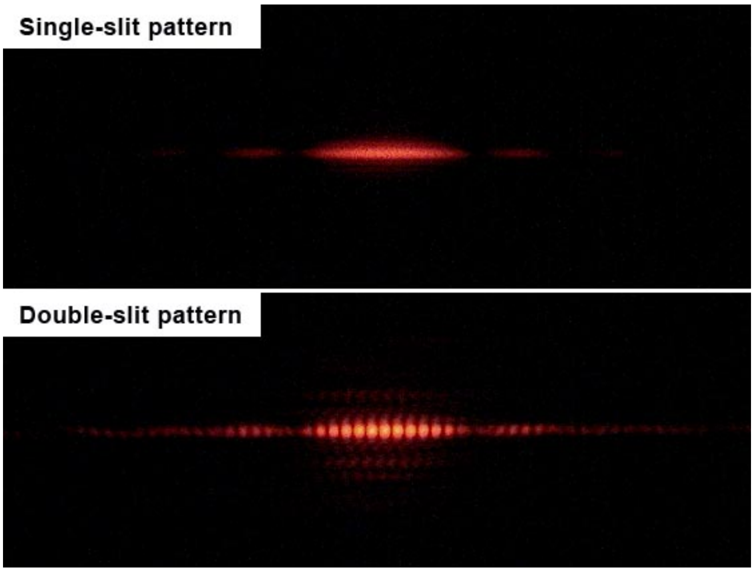

Figure 2.3: *Diffraction pattern behind single slit and double slit [17]*

2.3 From light wave to diffraction pattern

2.3.1 The Scalar Wave Equation of Light

Light is an electromagnetic wave. This was first proven by James Clerk Maxwell with his Maxwell's equations. In a dielectric medium that is linear, isotropic homogeneous and non-dispersive, all components of the EM field behave in the same way and their behavior can be described by a single scalar wave equation:

$$\nabla^2 u(\mathbf{r}, t) - \frac{n^2}{c^2} \frac{\partial^2 u(\mathbf{r}, t)}{\partial t^2} = 0 \tag{2.6}$$

In this equation $u(\mathbf{r}, t)$ may represent any of the components of the electric ($\mathbf{E}$) and magnetic ($\mathbf{H}$) field at position $\mathbf{r}$ and time t. n is the refractive index of the medium and c the speed of light in vacuum. Of course, in most cases the requirements of an isotropic, non-dispersive, homogeneous, dielectric media aren't met. Therefore, the representation of the wave equations in scalar form is seen as an approximation [5]. In our case, diffraction of light by an aperture, the (**E**) and (**H**) fields are only modified at the edges of the aperture where the light interacts with the material of the edges. This effect extends only over a few wavelengths. So, if the aperture is larger than the wavelength of the light, the effects will be small, and we can assume homogeneous media.

Equation 2.6 is the time-dependent Helmholtz equation. The scalar field must be monochromatic, thus consisting of a single frequency. The scalar field can be written as:

$$u(\mathbf{r}, t) = A(\mathbf{r})\cos[\omega t + \phi(\mathbf{r})] \tag{2.7}$$

where $A(\mathbf{r})$ and $\phi(\mathbf{r})$ are the amplitude and phase of the wave at position $\mathbf{r}$. The angular frequency is represented by ω. In phasor representation this becomes:

$$u(\mathbf{r}, t) = Re[U(\mathbf{r})e^{jwt}] \tag{2.8}$$

U(P) equals $A(\mathbf{r})e^{\phi(\mathbf{r})}$ and is called the complex amplitude. Equation 2.8 must satisfy the scalar wave equation, and substituting this expression for u(**r**,t) into Eq. 2.6 yields:

$$(\nabla^2 + k^2)U(\mathbf{r}) = 0 \tag{2.9}$$

This equation is called the Helmholtz equation [6]. To get the diffraction pattern, we have to solve this equation for $U(\mathbf{r})$.

2.3.2 Green's Theorem

To solve the Helmholtz equation and find U(**r**), the Helmholtz equation will be converted into an integral using Green's theorem. Green's theorem involves two complex valued functions $U(\mathbf{r})$ and $G(\mathbf{r})$. It states the following: Let S be a closed surface surrounding volume V. If the first and second partial derivatives of $U(\mathbf{r})$ and $G(\mathbf{r})$ are single-valued and continuous, without any singular points within or on S (the sum of S_0 and S_1), Green's theorem states that [5]:

$$\iiint_V (G\nabla^2 U - U\nabla^2 G)\, dv = \iint_S (G\frac{\partial U}{\partial n} - U\frac{\partial G}{\partial n})\, ds \tag{2.10}$$

$\partial/\partial n$ is a partial derivative in the outward normal direction at each point of S. U corresponds to the wave field. There are multiple choices for $G(\mathbf{r})$ that yield a useful representation of diffraction. One is used by Kirchhoff in his Theory of Diffraction, and one is used by Sommerfeld in the Rayleigh-Sommerfeld Diffraction Integral discussed in this thesis [6].

2.3.3 Kirchhoff Integral Theorem

The Green function chosen in this theorem is a spherical wave given by:

$$G(\mathbf{r}) = \frac{e^{jkr_{01}}}{r_{01}} \tag{2.11}$$

here, $\mathbf{r}$ is the position vector from a point in the observation plane, P_0, to an arbitrary point in space, P_1. The distance from P_0 to P_1 is the corresponding distance, given by

$$r_{01} = \sqrt{(x_0 - x)^2 + (y - y_0)^2 + z^2} \tag{2.12}$$

This is illustrated in Figure 2.4.

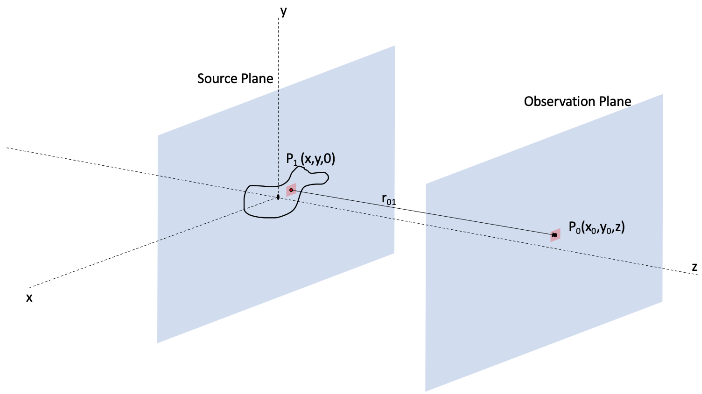

Figure 2.4: *Geometrical arrangement used in deriving Kirchhhoff's Integral Theorem.*

Both $U(\mathbf{r})$ and $G(\mathbf{r})$ satisfy the Helmholtz equation, thus the left hand side of Eq. 2.10 becomes

$$\iiint_V (G\nabla^2 U - U\nabla^2 G)\, dv = \iiint_V k^2[UG - GU]\, dv = 0 \tag{2.13}$$

This means that Eq. 2.10 can now be written as

$$\iint_S (G\frac{\partial U}{\partial n} - U\frac{\partial G}{\partial n})\, ds = 0 \tag{2.14}$$

Again, $\partial/\partial n$ is a partial derivative in the outward normal direction at each point of S. U corresponds to the wave field.The integral over S_0 goes to zero as the radius $R \to \infty$ if

$$\lim_{R\to\infty} R\left(\frac{\partial U}{\partial n} - jkU\right) = 0 \tag{2.15}$$

This is the Sommerfeld radiation condition and leads to results that correspond with experiments [6]. The only surface that remains in Eq. 2.14 is S_1, and the integral becomes

$$U(P_0) = \frac{1}{4\pi}\iint_{S_1}(G\frac{\partial U}{\partial n} - U\frac{\partial G}{\partial n})\,ds \tag{2.16}$$

Surface S_1 is an infinite opaque plane with any aperture denoted by A. Two approximations have to be made to determine the value of $U(\mathbf{r})$ on the surface of the aperture, these are called the Kirchhoff boundary conditions or the Kirchhoff approximation [1]. They state that U(x,y,z) and its partial derivative in the z-direction are discontinuous outside the aperture, and continuous inside the aperture (at z = 0). This leads to the following solution for $U(P_0)$, with the integral only over aperture A [6]:

$$U(P_0) = \frac{1}{4\pi}\iint_{A}\left(G\frac{\partial U}{\partial n} - U\frac{\partial G}{\partial n}\right)\,ds \tag{2.17}$$

Filling in our choice for Green's function:

$$U(P_0) = \frac{1}{4\pi}\iint_{A}\left(\frac{e^{jkr_{01}}}{r_{01}}\frac{\partial U}{\partial n} - U\frac{\partial}{\partial n}\left(\frac{e^{jkr_{01}}}{r_{01}}\right)\right)\,ds \tag{2.18}$$

2.3.4 Fresnel-Kirchhoff diffraction formula

The expression for $U(P_0)$ in Eq. 2.18 can be further simplified by assuming that the distance r_{01} between the aperture and observation point is many optical wavelengths.

$$\frac{\partial G(P_1)}{\partial n} = \frac{\partial}{\partial n}\left[\frac{e^{jkr_{01}}}{r_{01}}\right] = \cos(\theta)\left[jk - \frac{1}{r_{01}}\right]G(P_1) \cong jk\cos(\theta)G(P_1) \tag{2.19}$$

Substituting this approximation in Eq. 2.18, we find [6]:

$$U(P_0) = \frac{1}{4\pi}\iint_{A}\frac{e^{jkr_{01}}}{r_{01}}\left[\frac{\partial U}{\partial n} - jk\cos(\theta)U\right]\,ds \tag{2.20}$$

Now, suppose that the aperture is illuminated by a single spherical wave originating at a point P_2. The distance between P_1 and P_2 is r_{21}, the angle between $\mathbf{n}$ and $\mathbf{r}_{21}$ is θ_2.

$$U(P_1) = G(r_{21})\frac{e^{jkr_{21}}}{r_{21}} \tag{2.21}$$

$$\frac{\partial U(P_1)}{\partial n} \cong jk\cos(\theta_2)G(r_{21}) \tag{2.22}$$

Filling this into Eq. 2.20 yields the following result:

$$U(P_0) = \frac{1}{j\lambda}\iint_A \frac{e^{jk(r_{21}+r_{01})}}{r_{21}r_{01}}\left[\frac{\cos(\theta)-\cos(\theta_2)}{2}\right] ds \tag{2.23}$$

This result is known as the Fresnel-Kirchhoff diffraction formula. It is valid for the diffraction of a spherical wave by a plane aperture [6].

2.3.5 Rayleigh-Sommerfeld Diffraction Formula

Kirchhoff's theory has yielded impressive experimental results and is widely used. However, there are certain inconsistencies in this theory caused by imposing Kirchhoff's boundary conditions on both the field strength and its normal derivative. If a two-dimensional potential function and its normal derivative vanish along any finite curve segment, then the potential function must vanish over the entire plane. The same holds for a three-dimensional wave equation, if it vanishes on any finite surface element, it must vanish in all space. In other words, Kirchhoff's boundary conditions say that the field is zero behind the aperture, which we know contradicts the physical situation [5]. Also, the Fresnel-Kirchhoff diffraction formula for a spherical wave fails to recreate the boundary conditions when the observation point is closer to the aperture.

These inconsistencies were later removed by Sommerfeld with the use of another Green's function. We start again with Eq. 2.16. This equation is valid if the scalar theory holds, both U and G satisfy the homogeneous scalar wave equation and the Sommerfeld radiation condition is satisfied [5]. The following Green's function is used by Sommerfeld:

$$G_2(\mathbf{r}) = \frac{e^{jkr_{01}}}{r_{01}} - \frac{e^{jk\underline{r_{01}}}}{\underline{r_{01}}} \tag{2.24}$$

r_{01} is the distance from $\underline{P_0}$ to P_1, and $\underline{P_0}$ is the mirror image of P_0 with respect to the initial plane. $\underline{r_{01}}$ is the mirror function of r_{01}, thus the distance from P_0 to $\underline{P_1}$. Filling $G_2(\mathbf{r})$ into Eq. 2.16 gives us the first Rayleigh-Sommerfeld diffraction formula [6]:

$$U(x_0, y_0, z) = \frac{1}{j\lambda}\iint_{-\infty}^{+\infty} U(x, y, 0)\frac{z}{r_{01}}\frac{e^{jkr_{01}}}{r_{01}}\, dx\, dy \tag{2.25}$$

In some textbooks such as Introduction to Fourier Optics from the McGawhill Electrical and Computer Engineering Series [5], $\frac{z}{r_{01}}$ is replaced by $\cos\theta$, where θ is the angle between the vectors $\mathbf{n}$ and $\mathbf{r}_{01}$. Eq. 2.25 shows that $U(x_0, y_0, z)$ can be interpreted as a linear superposition of diverging spherical waves, spreading out from a point (x,y,0) in the aperture weighted by $\frac{1}{j\lambda}\frac{z}{r_{01}}U(x, y, 0)$. This is the mathematical form of the Huygens-Fresnel principle [1][6].

2.4 Further Approximations

Eq. 2.25 is often used to calculate diffraction. However, solving this integral analytically is almost impossible to do for all but simplified setups. Luckily, certain approximations can be applied to the Rayleigh-Sommerfeld diffraction integral to allow simpler calculations. They are only valid in certain regions, farther away from the aperture. The approximations we will consider are the Fresnel and Fraunhofer approximations. In Figure 2.5 the valid regions for the approximations are shown. Rayleigh-Sommerfeld is valid in the entire half-space to the right of the aperture, Fresnel is valid in the 'near field' and Fraunhofer in the 'far field' [6]. Exact bounds will be calculated below. Also, we will look at the calculation of Fresnel diffraction using a Fourier Transform, as we use this application later in our simulations.

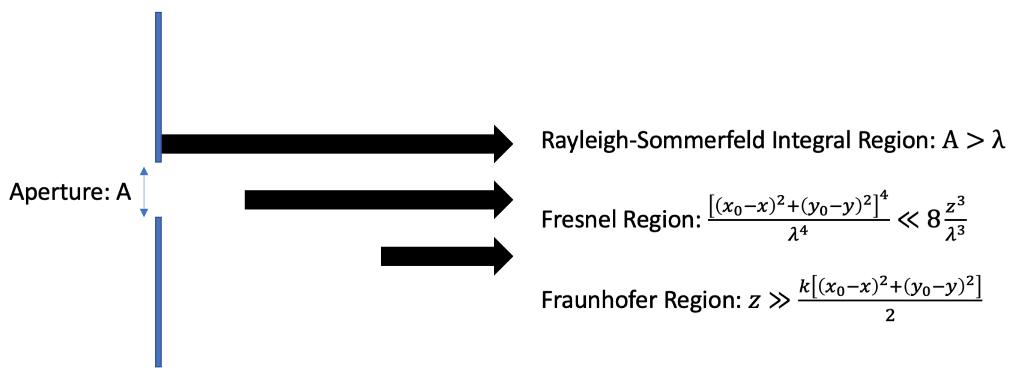

Figure 2.5: *The different regions where the Rayleigh-Sommerfeld integral, Fresnel and Fraunhofer are valid.*

2.4.1 Fresnel Diffraction

The first step towards the Fresnel diffraction integral is the paraxial approximation, stating that z is much larger than the aperture size [6]. Then we look at the biggest problem of Eq. 2.25, the expression for r_{01}

$$r_{01} = \sqrt{(x_0 - x)^2 + (y_0 - y)^2 + z^2} \tag{2.26}$$

We can simplify this by defining ρ and substituting it into the expression for r_{01}:

$$\rho^2 = (x_0 - x)^2 + (y_0 - y)^2 \tag{2.27}$$

$$r_{01} = \sqrt{\rho^2 + z^2} = z\sqrt{1 + \frac{\rho^2}{z^2}} \tag{2.28}$$

Now we use the binomial expansion for $\sqrt{1+b}$. This is given by:

$$\sqrt{1+b} = 1 + \frac{b}{2} - \frac{b^2}{8} + ... \tag{2.29}$$

We can now express r_{01} as

$$r_{01} = z\left[1 + \frac{\rho^2}{2z^2} - \frac{1}{8}\left(\frac{\rho^2}{z^2}\right)^2 + ...\right] = z + \frac{\rho^2}{2z} - \frac{\rho^4}{8z^3} + ... \tag{2.30}$$

If we use all terms of the binomial expansion, we don't make an approximation. So how many terms of the binomial expansion suffice? The answer depends on the occurrence of r_{01}. In the denominator of Eq. 2.25, the error of dropping all terms except the first one (z) is relatively small so we can say $r_{01}^2 \approx z^2$. However, for the r_{01} in the exponential, the errors are more substantial, since r_{01} is multiplied with k, a large value. Therefore, we need to retain the first and second term of the binomial expansion in the exponent [5]. The key to Fresnel approximation is assuming that the 3rd term is very small and thus can be left out. This is true if it is much smaller than the period of the complex exponential 2π:

$$k\frac{\rho^4}{8z^3} \ll 2\pi \tag{2.31}$$

Using the fact that $k = \frac{2\pi}{\lambda}$ we get the following relationship:

$$\frac{\rho^4}{\lambda^4} \ll 8\frac{z^3}{\lambda^3} \tag{2.32}$$

$$\frac{1}{\lambda^4}(x_0 - x)^2 + (y_0 - y)^2 \ll 8\frac{z^3}{\lambda^3} \tag{2.33}$$

If this condition holds for x, x_0, y, y_0 we can neglect third or higher order terms in the binomial expansion. For experimental setups using optical wavelengths λ, λ is often much smaller than the other physical dimensions: $\lambda \ll z$ and $\lambda \ll \rho$. This holds if $\rho \ll z$ and together with Eq. 2.31 marks the Fresnel region [6].

In this region we can then make the Fresnel approximation for r_{01}:

$$r_{01} \approx z + \frac{\rho^2}{2z} = z + \frac{(x_0 - x)^2 + (y_0 - y)^2}{2z} \tag{2.34}$$

Filling this into Eq. 2.25 for r_{01} together with $r_{01}^2 \approx z^2$ in the denominator we get the Fresnel diffraction integral:

$$U(x_0, y_0, z) = \frac{e^{jkz}}{j\lambda z} \iint_{-\infty}^{+\infty} U(x, y, 0) e^{jk[(x_0-x)^2+(y_0-y)^2]}\, dx\, dy \tag{2.35}$$

Another way to represent the Fresnel diffraction integral is through a Fourier Transform. We can numerically calculate this Fourier Transform much faster using the numpy.fft module [8]. First, we write out $(x_0 - x)^2$ and $(y_0 - y)^2$:

$$(x_0 - x)^2 = x_0^2 + x^2 - 2x_0 x \tag{2.36}$$

$$(y_0 - y)^2 = y_0^2 + y^2 - 2y_0 y \tag{2.37}$$

Now we can express the Fresnel diffraction integral as a two-dimensional Fourier Transform in k-space, using the following definition, where p, q are wave numbers like k:

$$G(p, q) = \mathfrak{F}[g(x, y)] \iint_{-\infty}^{+\infty} g(x, y) e^{-2\pi j(px+qy)}\, dx\, dy \tag{2.38}$$

We express the Fresnel diffraction integral as [6]:

$$U(x_0, y_0, z) = \frac{e^{jkz}}{j\lambda z} e^{\frac{j\pi}{\lambda z}(x_0^2+y_0^2)} \mathfrak{F}\left[U(x, y, 0) e^{\frac{j\pi}{\lambda z}(x^2+y^2)} \right]\Bigg|_{p=\frac{x}{\lambda z}, q=\frac{y}{\lambda z}} = h(x, y) \cdot G(p, q)|_{p=\frac{x}{\lambda z}, q=\frac{y}{\lambda z}} \tag{2.39}$$

It can be seen that the field strength U in the observation plane can be calculated by taking the Fourier transform of the product of the field distribution in the aperture $U(x, y, 0)$ and a quadratic phase function in the exponent.

2.4.2 Fraunhofer Diffraction

Now we consider a more rigid approximation, which, greatly simplifies the diffraction calculations when valid. This approximation is valid in the so-called far-field, or the Fraunhofer region. In addition to the Fresnel approximation which resulted in Eq. 2.35, we now make the stronger Fraunhofer approximation:

$$z \gg \frac{k[(x_0 - x)^2 + (y_0 - y)^2]}{2} \tag{2.40}$$

If this is condition is satisfied, we are far away from the aperture and we can ignore the quadratic terms in the exponent under the integral $e^{\frac{jk}{2z}[(x_0-x)^2+(y_0-y)^2]}$ because they are very small. Thus, the expression in the exponent becomes $e^{-\frac{jk}{2z}(x_0x+y_0y)}$ [5]. This gives us the following integral [6]:

$$U(x_0, y_0, z) = \frac{e^{jkz}}{j\lambda z} e^{\frac{jk}{2z}(x_0^2+y_0^2)} \iint_{-\infty}^{+\infty} U(x, y, 0) e^{-\frac{2\pi j}{\lambda z}(x_0x+y_0y)}\, dx\, dy \tag{2.41}$$

This can also explicitly be written as an integral over the aperture A:

$$U(x_0, y_0, z) \propto \iint_A U(x, y, 0) e^{-\frac{jk}{z}(x_0x+y_0y)}\, dx\, dy \tag{2.42}$$

Then one can clearly see that $U(x_0, y_0, z)$ is the 2D-Fourier transform of the field in the aperture plane $U(x, y, 0)$ at frequencies $p = \frac{x_0}{\lambda z}$ and $q = \frac{y_0}{\lambda z}$ [6]. Eq. 2.41 is the Fraunhofer diffraction integral and holds in the Fraunhofer region. A more elegant way to determine the minimal z-distance for this region is the "antenna designer's formula" [5].

$$z > \frac{2D^2}{\lambda} \tag{2.43}$$

In this equation, D is the largest dimension of the aperture $D = max(x^2 + y^2)$. If z meets this requirement, you are in the Fraunhofer region. Another way to make use of the Fraunhofer approximation if you don't have room in your experimental setup for a large D, is to view the diffraction pattern in the focal plane of a lens [2].

2.4.3 Fraunhofer Diffraction behind Double Slit

Now, let us consider the double slit as aperture (Figure 2.6) and analyze the resulting diffraction pattern using the Fraunhofer diffraction integral in one dimension. In 1D the Fraunhofer diffraction integral reduces to:

$$U(y_0, z) = \frac{e^{jkz}}{j\lambda z} e^{\frac{jk}{2z}y_0^2} \int_A U(y, 0) e^{-\frac{jk}{z}(y_0y)}\, dy \tag{2.44}$$

If we only address the relevant part of the integral and leave out the constants we get [7]:

$$\int_A e^{jky\sin\theta}\,dy = \int_0^a e^{jky\sin\theta}\,dy + \int_d^{d+a} e^{jky\sin\theta}\,dy \tag{2.45}$$

$$= \frac{1}{jk\sin\theta}\left(e^{jka\sin\theta} - 1 + e^{jk(d+a)\sin\theta} - e^{jkd\sin\theta}\right) = \left(\frac{e^{jka\sin\theta} - 1}{jk\sin\theta}\right)\left(1 + e^{jkd\sin\theta}\right) \tag{2.46}$$

$$U(y_0) = 2ae^{\frac{1}{2}jka\sin\theta}e^{\frac{1}{2}jkd\sin\theta}\frac{\sin[\frac{1}{2}ka\sin\theta]}{\frac{1}{2}ka\sin\theta}\cos\left(\frac{1}{2}kd\sin\theta\right) \tag{2.47}$$

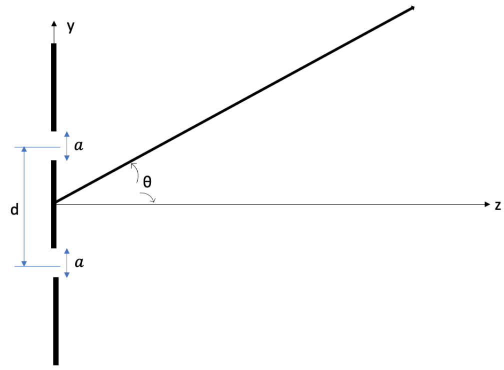

Figure 2.6: *Schematic drawing of double slit.*

To obtain the intensity I from U, we square the absolute value of U: $I = |U|^2$ [7]. The result we obtain is equivalent to the analytical formula for diffraction behind a double slit, Eq 2.5:

$$I(y_0) = I_0\left(\frac{\sin[\frac{1}{2}ka\sin\theta]}{\frac{1}{2}ka\sin\theta}\right)^2\cos^2\left(\frac{\pi d}{\lambda}\sin\theta\right)$$
$$= I_0\left(\frac{\sin[\pi a(\sin\theta)/\lambda]}{\pi a(\sin\theta)/\lambda}\right)^2\cos^2\left(\frac{1}{2}kd\sin\theta\right)$$

Chapter 3

Double Slit Experiment

Before starting on simulating the double slit experiment, we had perform the experiment physically. To make the virtual reality experience as close to the actual experiment, we determined the dimensions of the optical experiments, and calculate the parameters such as the slit width a and double slit distance d. In this chapter our experiment is discussed. How did we determine the parameters, and how do our results compare to the analytical formula?

3.1 Goal & Hypothesis

The goal of this experiment was to study the interference of light due to a double slit and see how each optical instrument influences the interference pattern. We also determine the parameters for the slit width a & distance between the slits d and compare the interference pattern to the analytical formula. The parameters determined in the physical experiment are used in the simulations.

We expect that the interference pattern is described by Eq.2.5. However, we expect that it may not entirely overlap due to misalignments. For example, if more light falls on one slit, we expect the maximum to shift towards the side of the more illuminated slit.

3.2 The Setup

The optical experiments in the virtual environment designed by VR Lab are based on the instruments used to build the setup. The setup is very straightforward. A laser pointer (frequency doubled Nd:YAG, $\lambda = 5.32 \cdot 10^{-7} m$), double slit, and CCD Alphalas (2048 pixels, pixel length = 14 μm) are placed on an optical rail [15]. One can find a schematic drawing of the setup in Figure 3.1. An extra screen is used to align the laser, this also has to be done in the VR application. A lens (f = 60 mm) is added between the double slit and the CCD or screen. The lens is used to determine the slit distance d and slit width a.

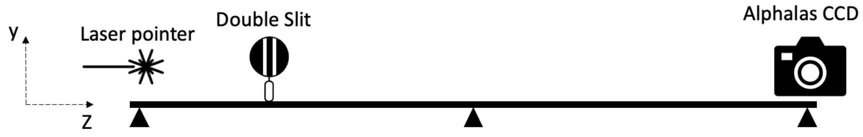

Figure 3.1: *Schematic drawing of the double slit experiment setup.*

3.3 Calculation of d and a

3.3.1 Measurement

When the distance between the lens and double slit is twice the focal distance of the lens $v = 2f$, one does not see a diffraction pattern on the screen, one simply sees two illuminated slits. The distance between these slits, and the width of these slits can be measured and used to calculate the actual d and a of the double slit. To do this, the lens formula and magnification formula are used.

$$\frac{1}{f} = \frac{1}{v} + \frac{1}{b} \tag{3.1}$$

$$N = \frac{b}{v} = \frac{B}{V} \tag{3.2}$$

In these equations, v is the distance between object and lens, b the distance between lens and image, f the focal distance, V the size of the object, and B the size of the image. We measured v and used it to calculate b with the lens formula. Then we calculated the magnification N. We could measure B on the screen, this was either the distance between the illuminated slits or the slit width. With this info, V was calculated. The formula for V is:

$$V(B, v, f) = \frac{1}{B\left(\frac{v}{f} - 1\right)} \tag{3.3}$$

This equation yielded the results found in Table 1.

v [mm]	σ_v [mm]	b [mm]	σ_b [mm]	N	σ_N [mm]	B [mm]	σ_B [mm]	V [mm]	σ_V [mm]
68	4	510	4	7.5	0.45	2.24	0.3	0.299	0.044
75	4	300	4	4	0.22	1.18	0.3	0.295	0.077
65	4	780	4	12	0.74	3.8	0.3	0.317	0.032
70	4	420	4	6	0.347	1.8	0.3	0.3	0.053

Table 3.1: *Measurements and calculations of V. In this case, V is the distance between the two slits: d. σ is the error in each measurement.*

The mean is taken of all values for V. This yields V or $d_experiment$ = 0.30 $\pm$ 0.05 mm. In Eq. 3.4 you find the formula we used to calculate the error.

$$\sigma_q(x, y) = \sqrt{\left(\frac{\partial q(x,y)}{\partial x}\sigma_x\right)^2 + \left(\frac{\partial q(x,y)}{\partial y}\sigma_y\right)^2} \tag{3.4}$$

In the same way, the slit width was calculated, now the width of a slit was measured on the screen at distance b. The results obtained are in Table 3.2.

v [mm]	σ_v [mm]	b [mm]	σ_b [mm]	N	σ_N [mm]	B [mm]	σ_B [mm]	V [mm]	σ_V [mm]
68	4	510	4	7.5	0.45	0.8	0.2	0.107	0.027
72	4	360	4	5	0.29	0.45	0.2	0.09	0.04
65	4	780	4	12	0.74	1.2	0.2	0.1	0.018
70	4	420	4	6	0.347	0.5	0.2	0.083	0.034

Table 3.2: *Measurements and calculations of V. In this case, V is the slit width: a. Again, σ is the error in each measurement.*

We again take the mean of the different results obtained for V and σ_V and this gives us a slit width $a_experiment$ = 0.10 $\pm$ 0.03 mm. Since the error margins are large compared to the obtained values for d and a, in the next section we will discuss the determination of d and a using a microscope.

3.3.2 Microscope

To more accurately determine the parameters d and a for the simulations, we measured them using a Nikon Japan Microscope. First, we determined the length of d and a in pixels, then converted the length in pixels to length in SI units by multiplying the length in pixels by the length of one pixel. To determine the length of one pixel, we had to calibrate the microscope. To do this, you measure a distance you already know, and measure the distance in pixels. This way you can calculate the pixel length. In order to determine the pixel length, we used a single slit with width a = 150 µm and a geo triangle with a = 1 mm = 1000 µm. We measured the width of both objects at multiple locations and took the average of these measurements.

The pixel length based on the single slit was L_{ss} = 1.09 $\pm$ 0.02 µm. The pixel length based on the geo triangle was L_{geo} = 1.05 $\pm$ 0.03 µm. To determine the error in pixel length, Since the different calibration objects yielded us different pixel lengths, we got two different values for d and a of the double slit. These values can be found in Table 3.3.

Calibration	d [µm]	a [µm]
Single slit	349 $\pm$ 6.8	54 $\pm$ 2.4
Geo triangle	336 $\pm$ 3.1	52 $\pm$ 2.1

Table 3.3: *Results for slit distance d and slit width a obtained with geo triangle and single slit calibration.*

The results for d and a obtained with the two calibration methods are not the same. Therefore, we take the average of the two results and propagate the error. We again used Eq. 3.4 to calculate the error in our final result. We concluded that d = 343 $\pm$ 3.7 µm and a = 53 $\pm$ 1.6 µm.

We suspect that the difference in pixel length obtained via the different objects is caused by the distance between the microscope lens and object. In order to focus the lens on the object, we adjust the distance between the lens and said object. Hence the pixel length may vary. Also, we couldn't get the two slits of the double slit in focus at the same time. This might be because the slits are not perfect. One slit might be deeper than the other one. We think that these factors contribute to the error in our findings.

At the first glance, it seems odd that d and a don't have perfectly rounded dimensions. However, the double slit and many other optical instruments used in the Bachelor Lab, are made by the Leidse Instrumentmakers School specifically for the Physics program and they slightly varied the size of the instruments so not all students get exactly the same results when conducting their experiments. Thus, our obtained results for d and a are valid, and we will use these as our parameters in our simulations. We will use the results for d and a obtained with the microscope, since these are more accurate.

3.4 Interference pattern

The next step in our experiment was to determine the interference or diffraction pattern. To look at said pattern, we used the CCD Alphalas webcam application. In this application, the signal of each pixel is plotted. In Figure 3.2 you can see the interference pattern caused by the double slit aperture. The distance between the double slit and CCD was 79 cm. In the left plot, the raw data is plotted. In the right plot, the noise is reduced by subtracting the mean of the captured noise data. The x-axis was transformed from pixels to µm, by multiplying the array containing the data points for the x-axis with the pixel length of 14 µm. Lastly, we normalized the intensity by dividing it through the maximum intensity, in order to be able to compare it more easily to future simulations and the analytical formula for the diffraction pattern.

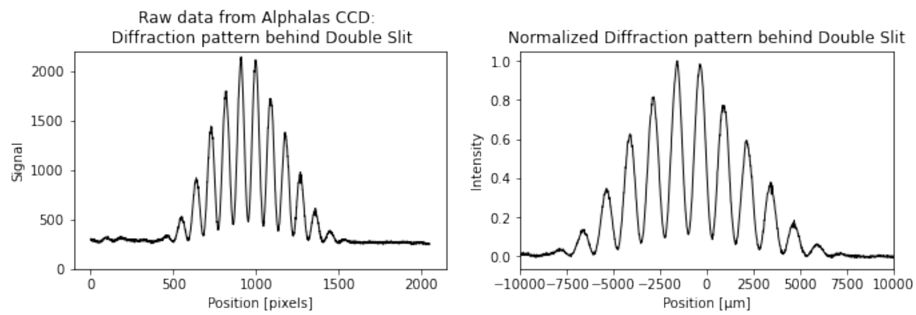

Figure 3.2: *Diffraction pattern behind double slit. In both plots, the distance between double slit and CCD camera R = 79 cm. Parameters d = 343 µm, a = 53 µm. The left plot is the raw data. The right plot shows the same data with noise reduction, normalized intensity and the position in µm on the x-axis.*

In Figure 3.2 one can see that the interference pattern isn't perfectly centered around x = 0. This is due to a misalignment of the double slit or laser pointer. The double slit is slightly rotated, so one slit is closer to the light source than the other. This causes a different phase of the light from the two slits. One can observe this even more clearly in Figure 3.3. Here the normalized interference pattern obtained through the CCD and the analytical formula (Eq. 2.5) are plotted in the same plot along the same axis. However, we substituted $\sin\theta$ by x/R in order to get the same x-axis. In this plot, one can also see that the minimums of the experimental interference pattern don't go to zero, while they do in the analytical formula. We suspect that this is also due to imperfections in our setup, such as misalignments and the manufacturing of the double slit.

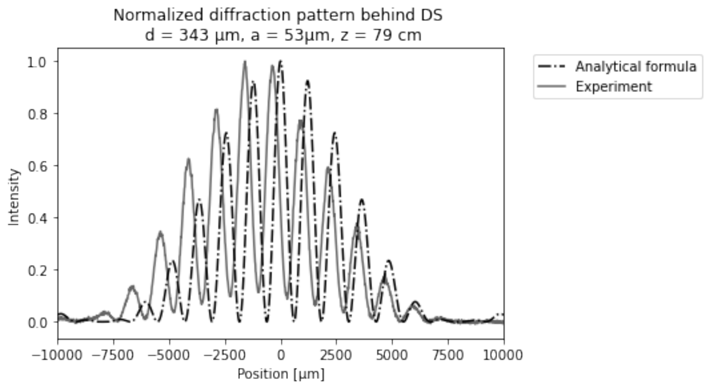

Figure 3.3: *Comparison of experimental result and analytical formula (Eq. 2.5) for diffraction pattern. The parameters are* $d = 343\,\mu m$*,* $a = 53\,\mu m$*,* $R = 79\,cm$*,* $\lambda = 5.32 * 10^{-7}$ *m.*

Chapter 4

Simulations

In this chapter the simulations of the double slit experiment are discussed. First we will look at simulations made with the library Diffractio [13], a diffraction-interference module for python. In this module, we used the Rayleigh-Sommerfeld diffraction integral to calculate the diffraction pattern. Then, we will discuss our own simulations, we implemented the Fresnel approximation, and converted it to a FFT. We will also look at the 2D FFT of the Fresnel approximation.

4.1 Diffractio

We mainly used Diffractio to check whether our own simulations were going in the right direction. Also it was a good example on how to proceed with the sort of calculations needed. For example, we had to calculate a double integral over two planes; the source plane and the observation plane. These integrals can take a long time and for the application of our project, it is vital to make the simulations as fast as possible.

We will not be comparing the Diffractio results to our experimental results, since it would be unnecessary since we will compare the experimental results to our own simulations in the next subsections. What we will discuss this section, is the simulation of light sources in Diffractio and double slit. Then, we will look at the diffraction pattern at different distances from the double slit. Next, we will include a lens and observe the diffraction pattern in the Fraunhofer region. Lastly, we will summarize the main takeaways important for our own simulations.

4.1.1 The Light Sources and Double Slit

The light sources we used in our simulations were a plane wave and a Gaussian beam. According to Brooker's Modern Classical Optics [3]: "A Gaussian beam is a beam of light whose profile varies in a Gaussian way with radial distance from its central axis." A Gaussian beam is important for our simulations because the output of a laser is often of the form of a Gaussian beam. In Figure 4.1 one can see the two different light sources made using Diffractio. The wavelength used is $\lambda = 532$ nm, the same as in the actual experiment. The functions used for the light sources can be seen below.

Formula for plane wave:

```
A*exp(1j*k*(self.x*sin(theta) + z0*cos(theta)))
```

Formula for Gaussian beam:

```
gausbeam0.gauss_beam(x0, w0, z0, A=1, theta=0.0)
```

For both sources, we used the following parameters: k = $2\pi/\lambda$, $\theta = 0$ (the incident angle of the wave), $z0 = 0$. The array x is the x-axis we use to create the light source. Here, 2000 µm with 8192 data points. We give both sources an amplitude A of A = 1. In addition, w0 = 300 µm, this is width of the Gaussian beam at z = 0.

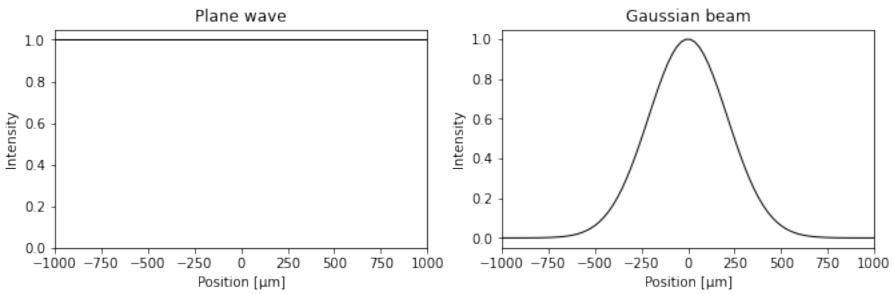

Figure 4.1: *Light sources in Diffractio.*

For the aperture function we used a double slit mask. We assigned the following parameters:

- The distance between the slits: d = 80 µm.
- Slit width a = 30 µm.
- Range: the same x-array used in the source.

It is important to note that the aperture plane, source plane and observation plane are all the same size, and contain the same number of data points. This is disadvantageous because the greater the distance between the source plane and observation plane, the wider the diffraction pattern becomes and the greater our x-array needs to be. This leads to slower calculations and sometimes plotting errors since the Diffractio algorithms can't handle the amount of data points.

4.1.2 The Diffraction Pattern

We chose to calculate the diffraction patterns with the Rayleigh-Sommerfeld algorithm Diffractio offers. The function for the light source is multiplied with the aperture function and results in an array we named `uds`. Then, the Rayleigh-Sommerfeld algorithm is applied using a given distance z. As you can see in Figure 4.2, the diffraction pattern greatly varies at different distances from the aperture. At the distance of z = 5 mm, the pattern looks nothing like the analytical formula. The more the distance increases, the pattern looks like the pattern in the Fraunhofer region.

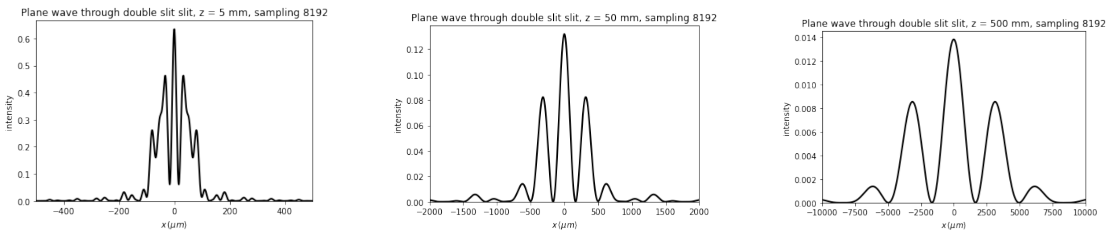

Figure 4.2: *Diffraction pattern behind double slit(d = 80 μm, a = 30 μm) at different distances from the aperture, illuminated with plane wave.*

You can also observe in figure 4.2 that the diffraction pattern widens as the distance increases. That is why we adjusted the x-axis accordingly. Furthermore, Diffractio does calculate the intensity, and you can see that the greater the distance z, the lower the intensity. The diffraction patterns farther away from the aperture have the same form as the analytical formula Eq 2.5, with a sinc-function as envelope. However, because the slit width a and slit distance d are smaller than in the experiment, less maximums are present.

4.1.3 Adding a Lens: Fraunhofer Region

To look at the diffraction pattern in the Fraunhofer region, the far field, we add a lens and place the aperture in the focal point of the lens. The lens has a focal distance of f = 10 mm and a diameter of 5 mm. The lens gives the field incident to the lens a quadratic phases shift. This phase shift is depicted in the center image of Figure 4.3. The sawtooth function on the left and right side of the parabola are present because the phase shifts from π and $-\pi$.

The procedure of calculating the diffraction pattern with a lens present is a different from the method explained in the previous section. The part where the light source array is multiplied with a mask of the aperture remains unchanged. Then, a new mask is created: the lens. You can give this lens your desired parameters: focal length, diameter, and wavelength. You multiply your lens mask with `uds` : `uds_lens = uds*tlens`. You fill in at what distance z you want to calculate the diffraction pattern, and apply the Rayleigh-Sommerfeld algorithm to `uds_lens`.

On the right side of Figure 4.3 you can see the diffraction pattern when the double slit aperture is placed in the focal plane of the lens. This is part of the Fraunhofer regime. If you look back at Eq. 3.1, you can see that if the distance between the aperture and lens (v) is equal to the focal length (f), the distance to the image of the aperture (b) is infinite. Thus, the right side should match the plot of the analytic formula.

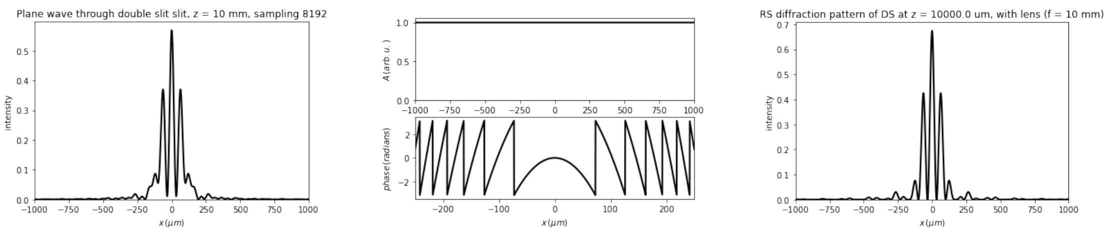

Figure 4.3: *Diffraction pattern behind double slit(d = 80 μm, a = 30 μm), illuminated with plane wave. Left image is diffraction pattern without lens at a distance of z = 10 mm, the middle image shows the amplitude and phase of the lens, and the right image shows the diffraction pattern when the double slit aperture is placed in the focal plane of the lens.*

4.2 Own Simulations

There are many ways to calculate the diffraction pattern behind an aperture. In this section two approaches are discussed. First we will look at our implementation of Fresnel diffraction using Eq. 2.35. We only consider the 1-dimensional scenario. Then, we examine the conversion of Fresnel diffraction into an Fourier transform, using the FFT module of NumPy [8]. This is done in two dimensions. We imported Numpy as `np`.

4.2.1 1D Fresnel Diffraction Integral Method

The most direct way to calculate the diffraction pattern is via Eq. 2.35. To examine the method, we will discuss the creation of light sources, double slit and diffraction pattern we obtained.

Creation of Light Source and Double Slit

Just like the Diffractio simulations, the light source was either a plane wave or a Gaussian beam. We created functions for the Gaussian beam, plane wave and double slit. The plane wave has the same form and parameters as the plane wave from Diffractio [13]. The Gaussian beam was defined as a Gaussian function:

$$U_{gb} = e^{-\left(\frac{x-\mu}{\sigma}\right)^2} \tag{4.1}$$

The maximum amplitude is one by default. σ is normally the standard deviation, but also determines the width of the curve. We took σ = 200. μ determines the location of the maximum, and we took μ = 0 as default. Furthermore, x is an array containing the data points at the source plane, defined as follows:

```
size = 20000
ndatapoints = 2048
x = np.linspace(-size/2, size/2, ndatapoints)
```

Here, `size` is the length of the array in µm. `ndatapoints` speaks for itself.

The aperture in question is of course a double slit. We could define the slit distance d, slit width a. The plane containing the double slit has the same number of data points and has the same size as the source. The transmission of light (`x`) is 1 in the slits, and 0 everywhere else. We multiply the function defining the source plane with our double slit function `plane_wave()`, and is used to calculate the diffraction pattern at a later stage. This process is similar to the Diffractio algorithm, however, we don't use masks and classes, only functions.

The calculation so far is:

```
u_plane = plane_wave(0,0,x)
ds_aperture = double_slit(d = 343, a = 53, x)
u_ds_1 = u_plane * ds_aperture
```

Where `u_plane()` is a plane wave as light source without phase shift perpendicular to our optical axis z.

The Diffraction Pattern

The next step is to calculate the diffraction pattern. To do so, the inegral from Eq. 2.35 is defined in the following way:

```
import numpy as np
prefactor = 1/(1j*lamb)
u_fresneldif = np.zeros(len(xobserve), dtype='complex_')
for p in range(len(xobserve)):
    rfresnel = z + (xobserve[p]-x)**2/(2*z)
    u_fresneldif[p] = prefactor * np.sum( u_ds_1
    *(z/rfresnel**2) * np.exp(1j*k*rfresnel) )
```

An empty list is created and for each for-loop iteration over p in the length of array `xobserve` the position in the observation plane is calculated at distance z from the double slit. Then this value `rfresnel` is used to calculate the optical field at this position. The sum is taken over all the contributions of the field in the double slit plane to the optical field in the observation plane.

To get the intensity of the diffraction pattern, we take the absolute value of `u_fresneldif` and square it. To make comparisons to other methods easier, the results are normalized by dividing by the maximum value of array `u_fresneldif`.

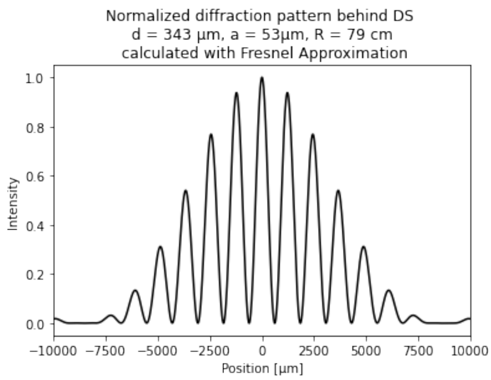

Figure 4.4: *Diffraction pattern behind double slit aperture, calculated using the Fresnel Approximation as integral.*

In Figure 4.4 the results are plotted of the above described method. The same parameters were used as determined in the experiment and at the same distance z = R.

4.2.2 2D Fresnel FFT Method

The previous method delivered correct results and can be used to calculate the diffraction pattern at all distances from the double slit in the Fresnel region. Nonetheless, the for-loop used to calculate the integral takes a while, and is too slow for more data points. Therefore, it cannot be converted to 2 dimensions. Thus, another method is needed. Since the Fresnel diffraction integral after applying the Fresnel approximation can be converted into a Fourier transform, we used the FFT module of NumPy to make simulations of the diffraction pattern in 2D [8]. In addition to the use of NumPy and matplotlib, SciPi packages misc and ndimages are also used [11].

Creation of Light Source and Double Slit

The function for the light source in 2D is created using a similar formula to the Diffractio module [13]. However, in our own simulation no classes and masks are used. The double slit is created out of two single slits, inspired by Rafael de la Fuentes simulations [4]. The function that creates the Gaussian beam works as follows:

```
import numpy as np
def gaussian_beam2D(x, x0, y, y0, w0, z0, A, phi, theta):
    global k
    x0 = int(x0 + z0*np.sin(theta))
    y0 = int(y0 + z0*np.sin(phi))
    w0x = w0
    w0y = w0
    z_rayleigh = k * w0x**2 / 2
    alpha = np.arctan2(z0, z_rayleigh)
    wx = w0x * np.sqrt(1 + (z0/z_rayleigh)**2)
    wy = w0y * np.sqrt(1 + (z0/z_rayleigh)**2)
    w = np.sqrt(wx*wy)
    if z0 == 0:
        R = 1e10
    else:
        R = z0 * (1 + (z_rayleigh / z0)**2)
    amplitude = A * w0/w * np.exp(-(x-x0)**2/
        (wx**2) - (y+y0)**2/(wy**2))
```

```
    phase1 = np.exp(1j*k)
    phase2 = np.exp(1j * (k*z0 - alpha + k*(x**2+y**2)/(2*R)))
    u_gaussian = amplitude * phase1 * phase2
    return u_gaussian
```

The input parameters `x` and `y` are coordinate matrices from coordinate vectors. `(x0,y0)` are the coordinates from the origin, If you want the beam centered, these are both equal to 0. `w0` is the beam width in the origin `(x0,y0)`, and `z0` is the position of the Gaussian beam along the z-axis. In the center `(x0,y0)` the intensity has amplitude `A` = 1, and the intensity fades from the center. On the left side of Figure 4.5 the effect of `phi` and `theta` is shown. The origin `(x0,y0,z0)` remains the same, but the laser is tilted in a certain direction. For a perfectly aligned Gaussian beam, the parameters used are: `x0,y0, theta, phi` = 0, `z0` = 10^4 µm, and `w0` = 1500 µm. This corresponds to the values of `z0` and `w0` of the laser used in the experiment in Chapter 3 [15].

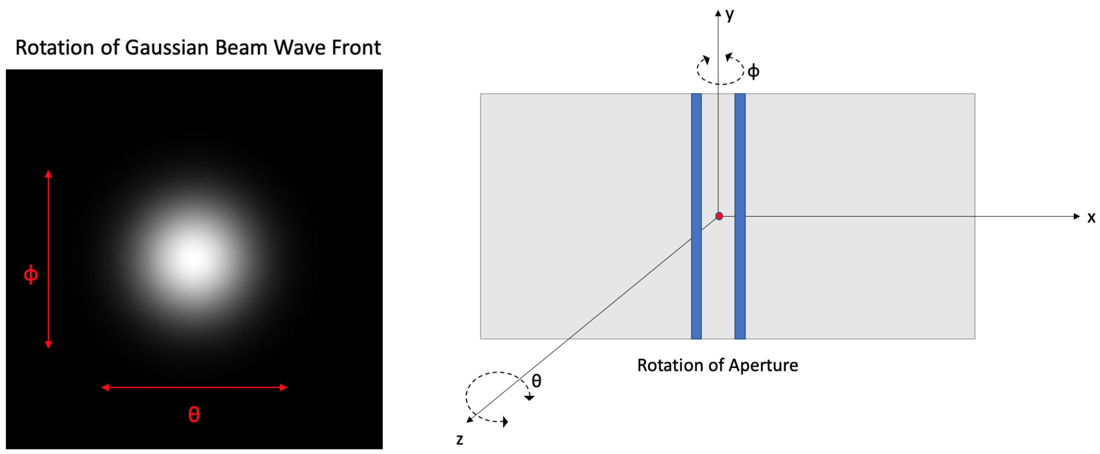

Figure 4.5: *The rotational planes of the Gaussian beam and double slit.*

As mentioned at the beginning of this section, the double slit is created by placing two single slits next to each other. They are placed next to each other with an equal distance from `x = 0`. The single slit transmits 100% within its own width, and transmits nothing of the light that falls on the opaque part. Below you see the function that creates the double slit: `double_slit2D()` from function `single_slit2D()`. Both contain the same amount of data points as the source plane and have the same dimensions.

```
import numpy as np
def double_slit2D(distance, height, xwidth, ywidth, phi, theta, x,y):
    global k
```

```
    double_slit = np.zeros((len(y), len(x)))
    double_slit += single_slit2D(x0=-distance/2, y0=-height,
        lx=xwidth, ly=ywidth, x=x, y=y)
    double_slit += single_slit2D(x0=distance/2, y0=-height,
        lx=xwidth, ly=ywidth, x=x, y=y)
    double_slit = ndimage.rotate(double_slit, theta, reshape=False)
    double_slit = double_slit * np.exp(1j*x*np.sin(phi)*k)
    return double_slit
```

The important parameters of this function are the distance between the two slits `distance` = 341 µm, slit width `xwidth` = 53 µm, length of a slit in y-direction `ywidth` = 8000 µm. Also, `(x,y)` are coordinate matrices from coordinate vectors with the same dimensions as `(x,y)` in the source plane. Furthermore, `phi` is the rotation about the y-axis. If `phi` $\neq 0$, one slit is slightly closer to the observation plane. Lastly, `theta` is the rotation about the z-axis, rotating the xy-plane, the rotation is done using the SciPy function `ndimage.rotate(double_slit, theta)` [11]. If `theta` $\neq 0$, the double slit is tilted. This is further illustrated on the right side of Figure 4.5.

The rotating of the double slit and Gaussian beam are crucial factors in recreating the experimental results. With these techniques, the misalignment of the double slit and laser can be replicated, creating more realistic simulations.

The Diffraction Pattern

In the same way as with the Fresnel approximation as integral, the source field is multiplied with the aperture:

```
    u = gauss2D_z * double_slit
```

Then, a Fast Fourier Transform (fft) is performed over this field `u` with `np.fft.fft2`, an algorithm to execute a 2D Fourier transformation in python. The function can be found below.

```
import numpy as np
def fresnelfft2D(u, z, xsource, ysource):
    global k, lambda
    prefactor1 = np.exp(1j*k*z) / (1j*lambda*z)
    prefactor2 = np.exp(1j*np.pi*(xscreen**2 + yscreen**2)/(lambda*z))
    fft_u = prefactor1* prefactor2*np.fft.fft2(u * np.exp(1j *
    k/(2*z) *(xsource**2 + ysource**2)))
    U = np.fft.fftshift(fft_u)
    return U
```

For `xsource` and `ysource` we again take the coordination matrices of the coordination vectors. For `z`, we take the distance from the double slit to the observation plane. The actual fft `fft_u` has the same form as Eq. 2.39. In order to center the x-axis properly, the fft has to be shifted using `np.fft.fftshift(fft_u)`. This makes x = 0 µm the center of the plots.

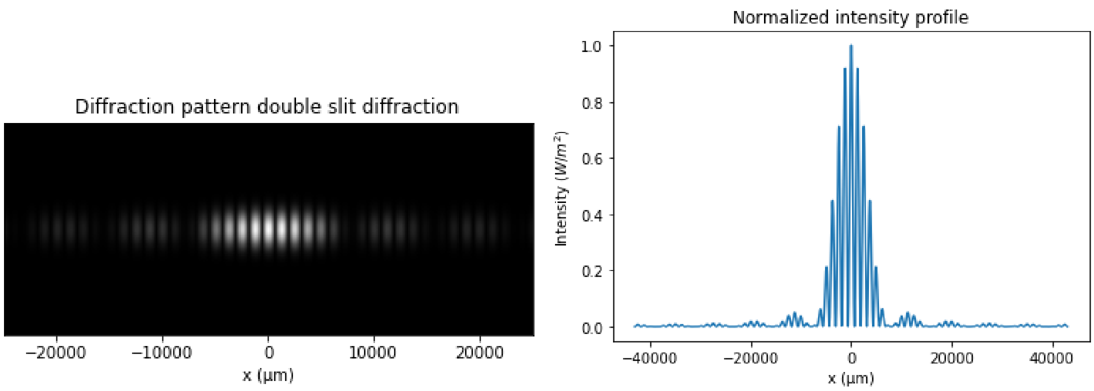

Figure 4.6: *Diffraction pattern behind double slit. The left side shows the 2D diffraction pattern, and the right side shows the normalized intensity profile. Number of data points = 2048, R = 79 cm, d = 343 µm, a = 53 µm, λ = 532 nm. The parameters for the Gaussian beam are the same as discussed in the previous section.*

The results of the 2D Fresnel FFT Method can be seen in Figure 4.6. Again, the same parameters are used as in the experiment. With this method, less data points are needed and a wider part of the diffraction pattern is calculated. Not only the first maximum of the sinc-envelope is plotted, also higher order maximums are present.

4.3 Comparison of Results

In the last section of Chapter 4, the results of the different simulations are compared to each other, and the Fresnel FFT method will be compared to the experimental results. Only this method is compared to the experimental results, since the rotation of the double slit and light source will give more realistic results. The Fresnel diffraction integral method will be compared to Diffractio and to Eq. 2.5. Then, the intensity profiles of the Fresnel diffraction integral method and Fresnel FFT method will be compared. Lastly, the Fresnel FFT simulation will be compared to the experimental data.

4.3.1 Diffractio vs. Fresnel Integral vs. Analytical Formula

In Figure 4.7 the intensity is plotted against the position on the screen in the observer plane. To plot the different methods in the same figure with the same x-axis, they all contain the same amount of data points (n = 8192). The wavelength $\lambda = 532$ nm, and the other parameters are named in the title. All methods are normalized in the same way by dividing through the maximum intensity. The results of the three different methods match well at a distance of R =10 cm, especially in the first maximums. But in the first sinc-envelope at $m = \pm 2$, the intensity is higher for the Diffractio result than for the analytical formula and the Fresnel integral. It is possible that this is due to the fact that the analytical formula and the Fresnel integral are approximations.

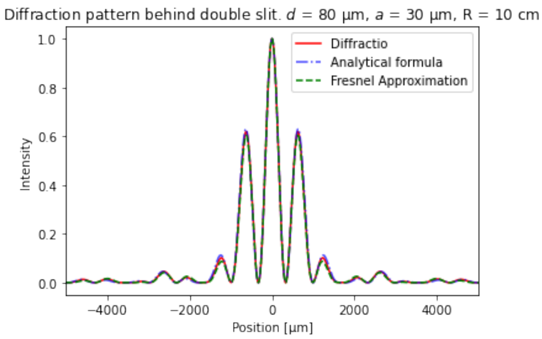

Figure 4.7: *Comparison of simulation with Diffractio module, Fresnel approximation and analytical formula (Eq. 2.5).*

4.3.2 Fresnel Integral vs. Fresnel FFT

Now, the two methods for our own simulations are compared. Since the FFT method is in 2D and the Fresnel integral is in 1D, we only look at the intensity of the diffraction pattern. We don't compare both methods to the experimental results, since the setup wasn't aligned properly and it was already established that there are some differences between the intensity of the experimental data and the intensity of Eq. 2.5. Since Eq. 2.2 and the Fresnel integral give similar results, we don't compare them to the experiment. However, for the default parameters for the 2D FFT method, the intensity patterns can be compared. The results are shown in Figure 4.8.

The locations of the minimum and maximums correspond, however, their intensities are higher in the pattern created using the Fresnel integral. We suspect

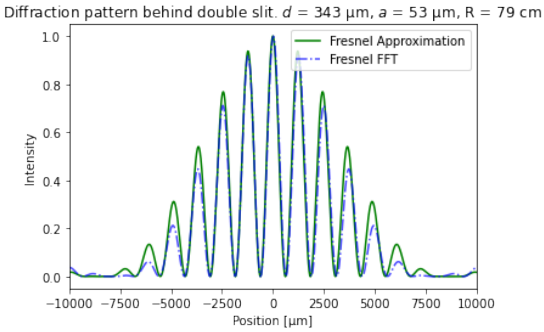

Figure 4.8: *Comparison of simulation with Fresnel FFT method and Fresnel approximation.d = 343 μm, a = 53 μm, R = 79 cm, λ = 532 nm. For the FFT light source rotation:* θ_{gb} *= 0 rad,* ϕ_{gb} *= 0 rad. For the FFT double slit rotation:* θ_{ds} *= 0 rad and* ϕ_{ds} *= 0 rad.*

that this is due to the fact that the intensity pattern from the 2D FFT method is calculated from a 2D array. Since the shape of the pattern is more important in our simulations than the intensity, both methods are still valid. Especially since the Fresnel integral only uses the matplotlib and NumPy module, and the FFT method also needs SciPy modules. Even though the FFT methods requires less data points, both methods take about the same amount of time to run. However, to more accurately simulate the experiment, the FFT method is preferred, since you can rotate the double slit. With the amount of datapoints needed for the Fresnel integral calculation, doing it in 2D would take too long for the VR Lab application.

4.3.3 Fresnel FFT vs. Experiment

Lastly we compare the Fresnel FFT to the experimental results. Since we can rotate the Gaussian beam and the double slit, we can replicate the diffraction pattern we obtained with our slightly misaligned setup, seen on the right side of Figure 3.2. In Figure 4.9, the Gaussian beam and double slit are slightly rotated and are a better fit to the experimental results. With our program, we can correct the double slit for the misalignment of the Gaussian beam. However, since both optical instruments were probably partly misaligned in our experimental setup, we also rotated both the Gaussian beam and double slit.

The simulation still doesn't perfectly replicate the experiment. The minimums of the simulations have a higher intensity than those of the experiment. Also, the intensity of some maximums is higher than in our simulation. But, the intensity of the two maximums in the middle match very well and the positions of the minimums and maximums coincide. The mismatch of the intensity can also be caused because of the way we reduced the noise. We subtracted the mean of the noise from our intensity array. The average noise was around $\sim$ 200, and the maximum intensity $\sim$ 4000, so we also reduced our maximum intensity by 200. This may have caused the higher intensity in the minimums. Of course, it is also possible that the double slit was even more misaligned than simulated.

Furthermore, there is still some noise present in the intensity of the experiment and not all pixels of the CCD camera capture the light completely. That is why some extremely sharp peaks are present in the experimental pattern. We also noticed some reflections of laser light from the metal aperture and attenuators in our setup. This may have also caused some unwanted interference.

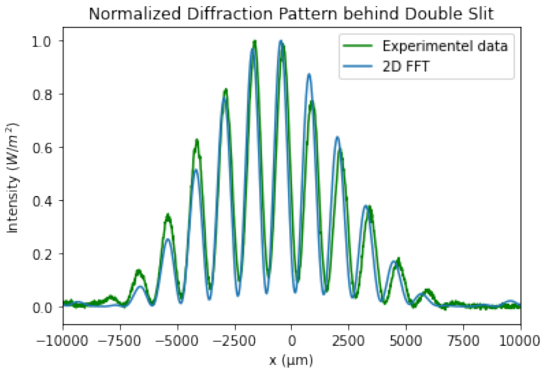

Figure 4.9: *Comparison of diffraction pattern created using 2D FFT method and experimental data. The parameters for both are: d = 343 μm, a = 53 μm, R = 79 cm, λ = 532 nm. For the FFT light source rotation: θ_{gb} = 0.015 rad, ϕ_{gb} = -0.08 rad. For the FFT double slit rotation: θ_{ds} = -2 rad and ϕ_{ds} = -0.006 rad.*

To conclude the comparison of the experiment to the simulation with the Fresnel FFT method, we can say that the rotation of the double slit and Gaussian beam results in a closer resemblance to the actual experimental results. Of course, there are still some factors that can be taken into account when creating a simulation, but the question is whether you want to include these in your simulation as most of them are unwanted in the actual experiment.

Chapter 5

Conclusion & Outlook

The goal of this Bachelor Research Program was to numerically calculate the diffraction pattern behind a double slit aperture. These calculations will be used by a company 'VR Lab' so that students can use these simulations to virtually prepare themselves for the actual experiment at the university. In order to achieve this goal, we studied several ways to calculate diffraction. We assumed the light used in our simulations was in a dielectric linear, isotropic, homogeneous and non-dispersive medium, thus the light could be described by a single scalar wave equation, and if the aperture is larger than the wavelength of the light, this scalar wave equation could be transformed into the Helmholtz equation. To solve the Helmholtz equation and come up with a value for $U(\mathbf{r})$, it is converted into an integral. This can be done using one of Green's functions. The Kirchhoff Integral Theorem uses the first Green's function, and to solve some inconsistencies, Sommerfeld later used a different Green's function. The Kirchhoff integral Theorem eventually yielded us the Fresnel-Kirchhoff diffraction formula, valid for the diffraction of a spherical wave by a plane aperture. Sommerfelds approach yielded us the Rayleigh-Sommerfeld diffraction formula, and after applying the Fresnel approximation and Fraunhofer approximation, we returned to the analytical formula.

In the physical experiment, the double slit distance $d = 343 \pm 3.7$ µm and slit width $a = 53 \pm 1.6$ µm were determined, and the diffraction pattern behind the aperture was obtained. Performing the actual experiment was an important step towards our goal, since it showed us what factors were important in simulating our data and showing us what to expect. The next step was to simulate the diffraction pattern using a python module Diffractio. This was mainly used to check whether our own simulations were correct. For our own simulations, we calculated the Fresnel integral using a for-loop, and we used the FFT-algorithm from NumPy to calculate the Fresnel diffraction as a Fourier transform. Both results corresponded with the Diffractio simulations. But because the second approach could be simulated in two dimensions, the double slit and Gaussian beam could be rotated. This leads to a closer resemblance to the experimental results.

Both methods can be used by VR Lab, their choice depends on the translation of our Python code to C++. The FFT method also used a SciPy module to rotate the instruments. Other important elements to consider in the further course of this project are the speed of the calculations and the magnitude of the intensity. using a for-loop takes a lot of time in python, and especially in virtual reality, you want to see an immediate result of your action such as moving the observation screen. The intensity of the diffraction pattern should also be improved. Because we normalized the intensity, this is not connected to the distance between the observation plane and aperture plane, but this is actually related to one another. Lastly, the implementation of a lens should also be implemented, both in one dimension as in two dimensions, since this is used to calculate the parameters of the double slit aperture in the experiment.

All in all, our simulations contribute to the understanding of the behaviour of light, and shows its wave-like nature. These simulations will hopefully help future 1st year physics students to further their knowledge and prepare their own experiment.

Acknowledgements

First, I would like to express my gratitude to Benjamin Claus. He worked on a similar project, and therefore we could work together on a daily basis. We always tried to help each other, and our daily talks helped me to deeper understand the theoretical concepts of diffraction and to apply them to the simulations.

I would also like to show my deep appreciation to my daily supervisor, Dr. Wolfgang Löffler, who guided me throughout this project. Dr. Löffler was always ready to aid Benjamin and me if we were stuck on a problem, and made room for us in his busy schedule. He challenged me to look further and to ask critical questions, therefore helping me improve my research skills. Dr. Löffler, thank you for giving me the opportunity to work in your research group, and for the educational project.

Then I would like to thank my second supervisor Dr.ir Paul Logman. His guidance was indispensable to gain insight into the physical experiment. Thank you for expanding my experimental knowledge! I also wish to acknowledge the help provided by Mirthe Bergman on the real life experiment. To everyone who helped my finalize this project, thank you.

Bibliography

[1] Bevan B Baker and Edward Thomas Copson. *The mathematical theory of Huygens' principle*, volume 329. American Mathematical Soc., 2003.

[2] Max Born and Emil Wolf. *Principles of optics: electromagnetic theory of propagation, interference and diffraction of light*. Elsevier, 2013.

[3] Geoffrey Brooker. *Modern classical optics*, volume 8. Oxford University Press, 2003.

[4] Rafael de la Fuente. Solving the diffraction integral with the fast fourier transform (fft) and python, 2020. [Online; accessed May 20, 2021], url = rafael-fuente.github.io/solving-the-diffraction-integral-with-the-fast-fourier-transform-fft-and-python.html.

[5] Giovanni De Micheli. Mcgraw-hill electrical and computer engineering series: Introduction to fourier optics.

[6] Okan K Ersoy. *Diffraction, Fourier optics and imaging*, volume 30. John Wiley & Sons, 2006.

[7] Grant R Fowles. *Introduction to modern optics*. Courier Corporation, 1989.

[8] Charles R. Harris, K. Jarrod Millman, Stéfan J. van der Walt, Ralf Gommers, Pauli Virtanen, David Cournapeau, Eric Wieser, Julian Taylor, Sebastian Berg, Nathaniel J. Smith, Robert Kern, Matti Picus, Stephan Hoyer, Marten H. van Kerkwijk, Matthew Brett, Allan Haldane, Jaime Fernández del Río, Mark Wiebe, Pearu Peterson, Pierre Gérard-Marchant, Kevin Sheppard, Tyler Reddy, Warren Weckesser, Hameer Abbasi, Christoph Gohlke, and Travis E. Oliphant. Array programming with NumPy. *Nature*, 585(7825):357–362, September 2020.

[9] Oliver S Heavens and Robert W Ditchburn. *Insight into optics.* 1991.

[10] Roger A. Freedman Hugh D Young. *University Physics with Modern Physics*. Pearson, 12th edition, 2016.

[11] Eric Jones, Travis Oliphant, Pearu Peterson, et al. SciPy: Open source scientific tools for Python, 2001–. [Online; accessed May 20,2021].

[12] Ariel Lipson, Stephen G Lipson, and Henry Lipson. *Optical physics*. Cambridge University Press, 2010.

[13] L.M. Sanchez Bre. Diffractio, python module for diffraction and interference optics.

[14] Algemeen Nederlands Persbureau. Universiteit leiden sluit deuren tot eind van academisch jaar, 2020.

[15] Thor Labs. *Nd:YAG Laser Mirrors, 2nd Harmonic*.

[16] Wikipedia, the free encyclopedia. Wave diffraction in the manner of huygens and fresnel, 2007. [Online; accessed June 8 2021].

[17] Wikipedia, the free encyclopedia. Results from the double slit experiment: Pattern from a single slit vs. a double slit., 2010. [Online; accessed June 1, 2021].

[18] Thomas Young. Experimental demonstration of the general law of the interference of light. *Philosophical Transactions of the Royal society of London*, 94(1804):1, 1804.